NÚREG/CR-3262
PNL-5515
Vol. 2

COBRA-NC:A Thermal Hydraulics Code for Transient Analysis of Nuclear Reactor Components

Vol. 2: COBRA-NC Numerical Solution Methods

Prepared by M. J. Thurgood, T. L. George, C. L. Wheeler

Pacific Northwest Laboratory
Operated by
Battelle Memorial Institute

Prepared for
U.S. Nuclear Regulatory Commission

NUREG/CR-3262
PNL-5515
Vol. 2
R4

COBRA-NC:A Thermal Hydraulics Code for Transient Analysis of Nuclear Reactor Components

Vol. 2: COBRA-NC Numerical Solution Methods

Manuscript Completed: March 1986
Date Published: April 1986

Prepared by
M. J. Thurgood, T. L. George, C. L. Wheeler

Pacific Northwest Laboratory
Richland, WA 99352

Prepared for
Division of Accident Evaluation
Office of Nuclear Regulatory Research
U.S. Nuclear Regulatory Commission
Washington, D.C. 20555
NRC FIN B2466

ABSTRACT

The COBRA-NC computer program has been developed to predict the thermal-hydraulic response of nuclear reactor components to thermal-hydraulic transients. The code solves the multicomponent, compressible three-dimensional, two-fluid, three-field equations for two-phase flow. The three fields are the vapor field, the continuous liquid field, and the liquid drop field. The code has been used to model flow and heat transfer within the reactor core, the reactor vessel, the steam generators, and in the nuclear containment. This volume describes the finite-volume equations and the numerical solution methods used to solve these equations. It is directed toward the user who is interested in gaining a more complete understanding of the numerical methods used to obtain a solution to the hydrodynamic equations.

CONTENTS

FIGURES

ACKNOWLEDGMENTS

COBRA-NC is the result of the efforts of a number of people. We wish to acknowledge the main contributors and to express our appreciation to those who have offered their advice and suggestions.

The main contributors to the program are listed below.

Fluid Dynamics:	M. J. Thurgood, T. L. George, and T. E. Guidotti
Heat Transfer:	J. M. Kelly and R. J. Kohrt
Turbulence Model:	K. R. Crowell
Graphics and Programming:	A. S. Koontz
Simulations:	R. J. Kohrt

We wish to thank Dr. T. Lee of the U.S. Nuclear Regulatory Commission for his patience, support, and suggestions during this large undertaking. We also wish to thank Drs. Lee, Tong, Shotkin, Han, and Zuber of the U.S. Nuclear Regulatory Commission and members of the Advanced Code Review Group for their many helpful suggestions. We also express our gratitude to our manager, Dr. D. S. Trent, for his support, and to Cathy Darby and Peggy Snyder for their roles in typing this report.

NOMENCLATURE

A	area
ALAT	area through which a vertical velocity convects transverse momentum
Cp	specific heat at constant pressure
$\underline{\underline{D}}$	deformation tensor
$\underline{\underline{D}}^*$	deleted deformation tensor
e	internal energy
E	error
F	mass flow rate
$\underline{F}$	total force due to viscous and turbulent shear stress
$\underline{\underline{F}}$	anisotropy tensor
FA	flow area for connection to the vessel
f	mass fraction
$\underline{g}$	gravitational acceleration
H	heat transfer coefficient
h	enthalpy
h_{fg}	enthalpy of vaporization
$\underline{i}$	unit vector in the x direction
$\underline{j}$	unit vector in the y direction
K	drag coefficient
$\underline{k}$	unit vector in the z direction
ℓ	mixing length
$\Delta\ell$	transverse length increment
$\underline{n}$	unit normal vector
NA	number of connections to top of mesh cell
NB	number of connections to bottom of mesh cell
NCA	number of connections to top of transverse momentum cell
NCB	number of connections to bottom of transverse momentum cell
NCH	number of channels
NDX	number of axial cells
NCON	total number of connections to a cell
NKA	number of connections to top half of vertical momentum cell

NKB	number of connections to bottom half of vertical momentum cell
NKII	number of transverse connections to the II face of a transverse momentum cell
NKJJ	number of transverse connections to the JJ face of a transverse momentum cell
NKK	total number of transverse connections to a scalar mesh cell
NG	number of transverse connections to a transverse momentum cell that are orthogonal to the transverse momentum cell velocity
NVCONIL	number of connections to the vessel in any one piping loop
P	pressure
q	interfacial heat flux
Q	sensible heat
S	width of transverse connection
S	source
S	net entrainment rate
T	turbulent and viscous shear stress terms
$\underline{\underline{T}}_T$	stress T = tensor
$\underline{\underline{T}}$	Reynolds stress tensor
Δt	time increment
U	vertical velocity
V	transverse velocity in Y direction
W	transverse velocity in Z direction
Δx	mesh vertical length increment

Greek Symbols

α	volume fraction
δ	linear variation of
Γ	net rate of vapor generation
γ	gap direction indicator; = +1 if channel is on upstream side of gap = -1 if channel is on downstream side of gap
ϵ	thermal diffusivity
ϵ_T	turbulent thermal diffusivity
ϵ_D	turbulent mass diffusivity

η	fraction of vapor generation coming from the entrained liquid
μ	viscosity
μ^T	turbulent viscosity
ρ	density
$\underline{\underline{\tau}}$	fluid-fluid stress tensor
τ_i	interfacial drag force

Subscripts

B	bulk property
C	condensation
c	continuity cell
CE	entrained drop mass error
CL	continuous liquid mass error
CV	vapor mass error
ce	source of entrained liquid mass
cℓ	source of continuous liquid mass
cv	source of vapor mass
CONV	convection area
D	deposition or de-entrainment
E	evaporation or entrainment
e	entrained drop phase
eℓ	liquid energy source
ev	vapor energy source
EL	liquid energy error
EV	vapor energy error
f	saturated liquid
g	saturated vapor
h	energy mixing length
I	counter on vertical stacks (channels) of computational mesh cells
i	interfacial
IA	counter on connections to top of transverse momentum cell
IB	counter on connections to bottom of transverse momentum cell
II	mesh cell on the upstream side of a transverse momentum cell

J	vertical level for scalar (mass, energy) mesh cell
j	vertical level for vertical momentum mesh cell
JJ	mesh cell on the downstream side of a transverse momentum cell
K	counter on transverse connections between vertical stacks of mesh cells
k	phase k
KA	counter on connections to top of mesh cell
KB	counter on connections to bottom of mesh cell
KJ	gap momentum cell average
L	counter on transverse connections to a cell
ℓ	continuous liquid phase
LA	counter on transverse connections to top of vertical momentum cell
LB	counter on transverse connections to bottom of vertical momentum cell
m	mixture property
m	momentum mixing length
m	momentum cell
me	entrained liquid momentum source
mg	combined steam and noncondensable gases
mℓ	continuous liquid momentum source
mv	vapor momentum source
p	pipe
r	relative velocity
sink	related to a pressure sink boundary condition
SCL	subcooled liquid
SCV	subcooled vapor
SHL	superheated liquid
SHV	superheated vapor
v	vapor phase
ve	drag between vapor and drops
vℓ	drag between vapor and continuous liquid
w	wall
ϕ	general phase subscript

Superscripts

n	new time value
o	old time value
T	turbulent
t	transpose
'	per unit length
*	donor cell

COBRA-NC: A THERMAL-HYDRAULICS CODE FOR TRANSIENT ANALYSIS OF NUCLEAR REACTOR COMPONENTS

VOLUME 2: COBRA-NC NUMERICAL SOLUTION METHODS

1.0 INTRODUCTION

The COBRA-NC computer program was developed to predict the thermal-hydraulic response of nuclear reactor components to small and large break loss-of-coolant accidents and other anticipated transients. It provides a two-component, two-fluid, three-field representation of two-phase flow. The two-component model allows the representation of water and its vapor as well as a noncondensable gas mixture. The noncondensable gas mixture may consist of any number of gas species. Each field is treated in three dimensions and is compressible. Continuous vapor/gas mixture, continuous liquid, and entrained liquid drop are the three fields. The conservation equations for each of the three fields and for heat transfer from and within the solid structures in contact with the fluid are solved using either a semi-implicit or implicit finite-volume numerical technique on an Eulerian mesh. COBRA-NC features extremely flexible noding for both the hydrodynamic mesh and the heat transfer solution. This flexibility provides the capability to model the wide variety of geometries encountered in vertical components of nuclear reactor primary systems.

The code has been assessed against a variety of two-phase flow data from experiments conducted to simulate important phenomena anticipated during postulated accidents and transients in light water nuclear reactor components.

The constitutive relations included in COBRA-NC comprise state-of-the-art physical models for the interfacial mass transfer, the interfacial drag forces, the liquid and vapor wall drag, the wall and interfacial heat transfer, the rate of entrainment and de-entrainment, and the thermodynamic properties of water and noncondensable gases. In addition, a mixing length turbulence model has been included as an option.

The documentation of the COBRA-NC program is presented in several volumes. Volume 1 contains a description of the basic three-field conservation equations and constitutive models used in the code.

Volume 2 contains a description of the finite-volume equations for the vessel and the numerical techniques used to solve these equations. Volumes 3 through 5 are the Users' Manuals that contain line-by-line input instructions for COBRA-NC and user guidance for application of the code. Volume 3 is the Users' Manual for General Two-Phase-Thermal Hydraulic Applications and explains all of the input data required for general application of the code. Volume 4 is the Users' Manual for Containment Analysis. It contains an explanation of the input data required for containment analysis only. It also provides examples of containment modeling procedures. Volume 5 is the Users' Manual for Flow Blockage and Hot Bundle Analysis and describes the input required for performing such analysis.

Volumes 6, 7, and 8 are the Assessment Manuals. They contain the results of simulations run to assess the performance of the code in each of the areas discussed above. Volume 9 is the Programmers Manual that explains COBRA-NC's working parts from a programmer's viewpoint. The structure of the code is described, and a narrative description of the function of each variable and subroutine in the code is given.

This volume, Numerical Solution Methods, describes the finite-volume equations and the numerical solution methods used to solve these equations. The finite-volume equations are presented in Sections 2.0 and 3.0. A semi-implicit numerical solution method is described in Section 4.0, and an implicit scheme is described in Section 5.0.

2.0 THREE-FIELD CONSERVATION EQUATIONS

The three-field conservation equations for multidimensional flow in COBRA-NC are presented in Volume 1 of this manual. The reader should refer to Volume 1 for a more complete discussion of these equations and a description of the physical models required for their closure. The finite-volume form of these equations will be presented here, and the term-by term correspondence between the conservation equations and the finite-volume equations will be pointed out.

Two numerical solution methods are available in the code: a semi-implicit method and an implicit method. The finite-volume equations shown in this section are written in the semi-implicit form. The differences between this semi-implicit form of the equations and the implicit form of the equations are explained in Section 4.0. When the semi-implicit form is used, the time step, Δt, is limited by the material Courant limit

$$\Delta t < \left|\frac{\Delta x}{V}\right| \tag{1}$$

where Δx is the mesh spacing and V is the fluid velocity. The implicit method has no numerically imposed time step limitations.

The finite-volume equations are written such that they may be solved on Cartesian coordinates, in lumped parameter form, or using the subchannel formulation in which some of the convective terms in the transverse momentum equations are neglected and idealistic assumptions are made concerning the shape of the transverse momentum control volumes.

The computational mesh and finite-volume equations are described using the generalized subchannel notations. These equations are equivalent to the three-dimensional Cartesian equations when the limiting assumptions of the subchannel formulation are not used and the mesh is arranged on a rectangular grid (see Volume 1, Section 2.0). All momentum flux terms are set to zero when the lumped parameter form is used.

2.1 Computational Mesh and Variable Placement

The equations are solved using a staggered-difference scheme where the velocities are obtained at the mesh cell faces and the state variables such as pressure, density, enthalpy, and void fraction are obtained at the cell center. The mesh cell is characterized by its cross-sectional area, its height, Δx, and the width of its connection with adjacent mesh cells, S. The basic mesh cell is shown in Figure 1. The basic mesh cell may be used to model any

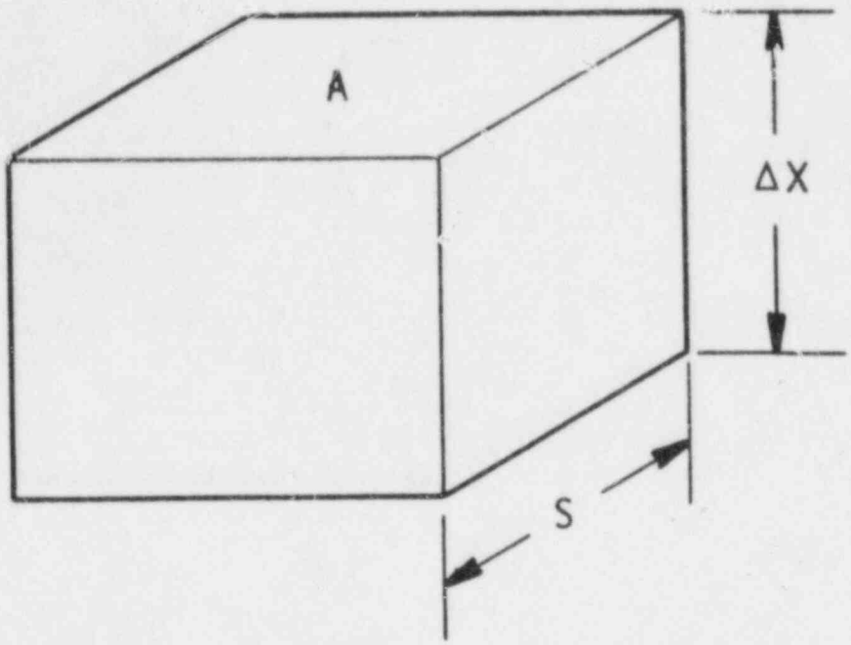

Figure 1 Basic mesh cell

one-, two-, or three-dimensional region. The dimensionality of the flow is dependent upon the number of faces on the cell that connect with adjacent mesh cells.

The size of a mesh cell used to model the flow field inside a reactor component is generally quite large because the volume of most reactor components is very large and the cost of using a fine mesh in solving the two-fluid equations for the whole component would be prohibitive. However, many important flow paths and flow phenomena may be overlooked when a large mesh size is used in some areas of the component. This can be minimized by allowing a variable mesh size within the component. A finer mesh can be used in areas where a more detailed calculation of the flow field is required. The code has been set up to allow such a variable mesh size. Examples of the flexibility this allows in modeling various geometries are given in the users' manuals (Volumes 3 through 5) and the applications manuals (Volumes 6 through 8). The variable mesh is formed by connecting two or more cells to any or all of the faces of a mesh cell, as illustrated in Figure 2. A single mesh cell with area A1 is shown connected to four mesh cells above it with areas A2, A3, etc. These four mesh cells may connect through transverse connections S2, S3, etc., to allow transverse flow in that region, or they may not connect to each other, forming one or more one-dimensional flow paths that connect to mesh cell 1. A more detailed discussion of the mesh is given in the users' manuals (Volumes 3 through 5). The mesh cells shown in Figure 1 and 2 represent the mesh for the scalar continuity and energy equations. The momentum equations are solved

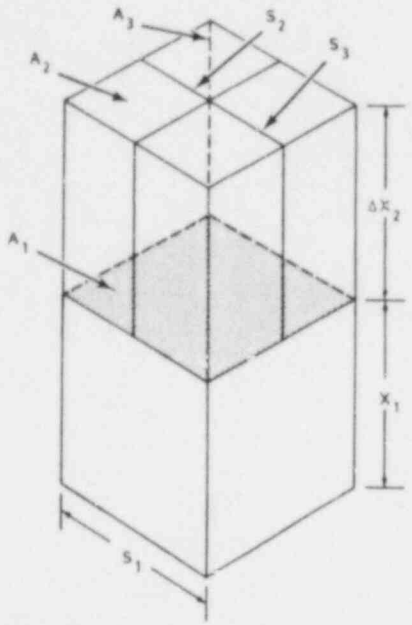

Figure 2 Variable mesh

on a staggered mesh where the momentum mesh cell is centered on the scalar mesh cell surface. The mesh cell for vertical velocities is shown in Figure 3, and that for transverse velocities in Figure 4.

The vertical velocities are subscripted with I and j where I identifies the location of the mesh cell within the horizontal plane and j identifies its vertical location. The mesh cells for the scalar equations carry the same subscripts, but their mesh cell centers lie a distance $\Delta x/2$ below the mesh cell center for the correspondingly subscripted velocity and are denoted by the capital letter J in the discussion below.

Transverse velocities are subscripted with k and J where k identifies the location of the mesh cell in the horizontal plane and J identifies its vertical location. The node centers for the scalar equations and transverse momentum equations lie in the same horizontal plane.

2.2 Finite-Volume Equations

In this section, the finite-volume equations are written in the semi-implicit form using the subscripting conventions described here. Quantities that are evaluated at the new time carry the superscript n and donor cell quantities carry the superscript *. Those quantities that have the superscript * or no superscript are evaluated at the old time and form the explicit portions of the equations.

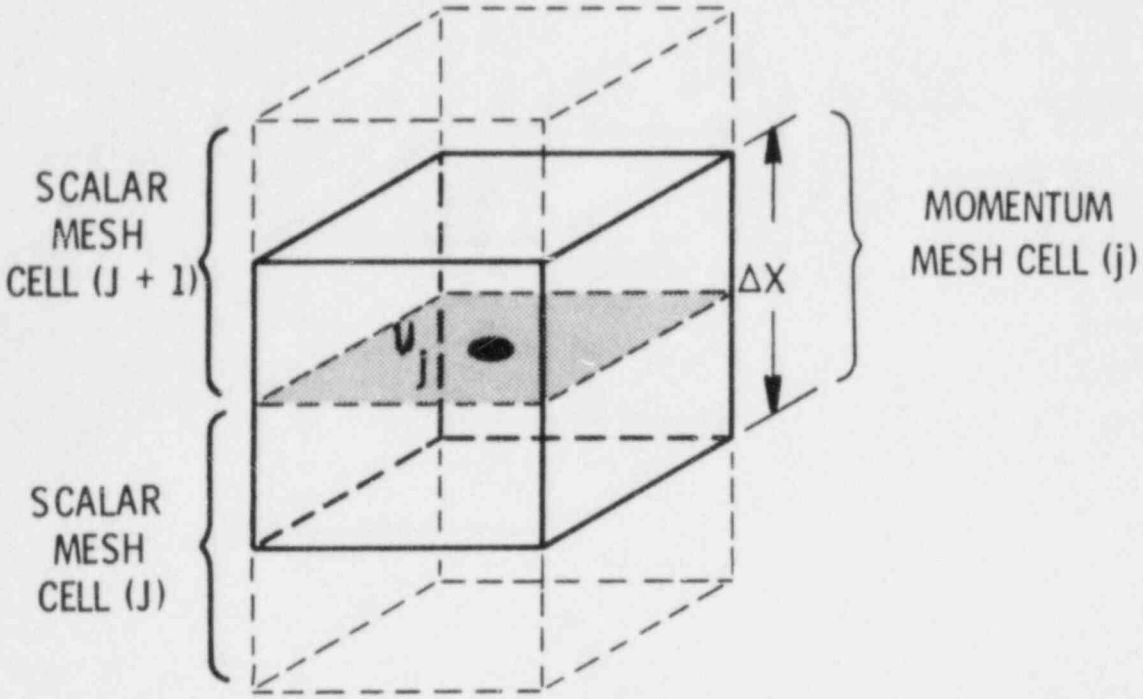

Figure 3 Mesh cell for vertical velocities

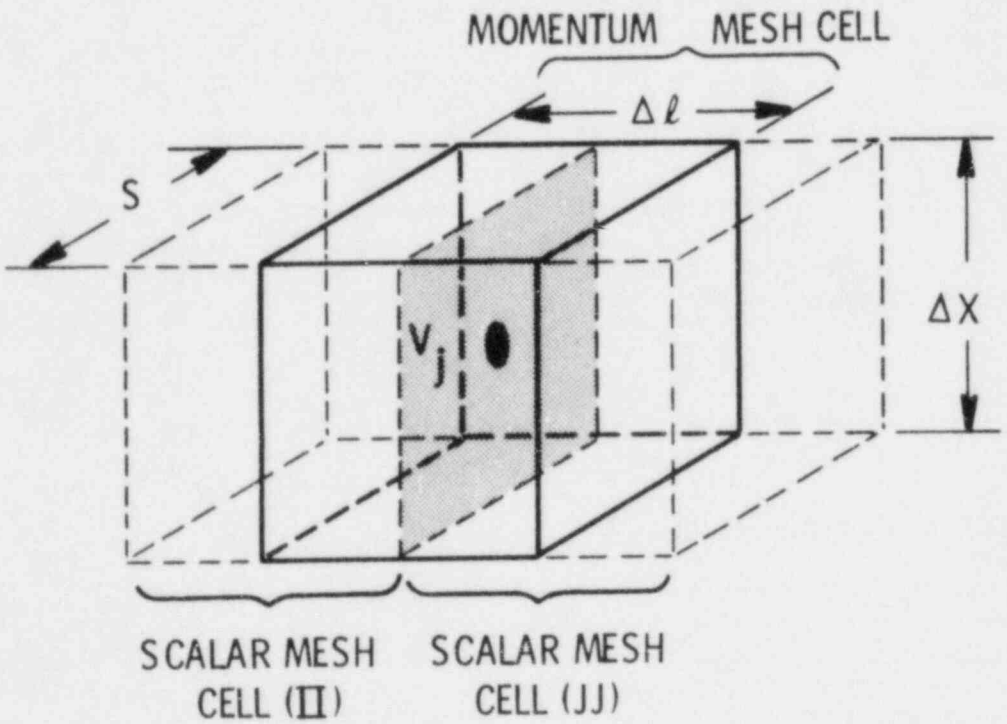

Figure 4 Mesh cell for transverse velocities

The corresponding term in the conservation equation for each term in the finite-volume equation is provided in the brackets below each equation, along with a verbal description of the term. The subscripts I and k are assumed to be obvious and are not shown.

2.2.1 Mass Equations

Gas Mixture Mass Equation

$$\frac{[(\alpha_v\rho_{mg})_J^n - (\alpha_v\rho_{mg})_J]}{\Delta t} A_{c_J} = \sum_{KB=1}^{NB} [(\alpha_v\rho_{mg})^* U^n_{vg_{j-1}} A_{m_{j-1}}]_{KB}$$

$$- \sum_{KA=1}^{NA} [\alpha_v\rho_{mg})^* U^n_{vg} A_{m_j}]_{KA} + \sum_{L=1}^{NKK} S_L \gamma[(\alpha_v\rho_{mg}) V_{vg_L}]_J \qquad (2)$$

$$+ \sum_{KB=1}^{NB} [(\alpha\rho_{vg})_{j-1} \epsilon_{D_{j-1}} (\frac{\rho_{mg_j}}{\rho_{vg_J}} - \frac{\rho_{mg_{J-1}}}{\rho_{vg_{J-1}}}) \frac{A_{m_{j-1}}}{\Delta x_{j-1}}]_{KB}$$

$$- \sum_{KA=1}^{NA} [\alpha\rho_{vg})_j \epsilon_{D_j} (\frac{\rho_{mg_{J+1}}}{\rho_{vg_{J+1}}} - \frac{\rho_{mg_J}}{\rho_{vg_J}}) \frac{A_{m_j}}{\Delta x_j}]_{KA}$$

$$- \sum_{L=1}^{NKK} \gamma(\alpha\rho_{vg})_{LJ} \epsilon_{D_L} (\frac{\rho_{mg_{II}}}{\rho_{vg_{II}}} - \frac{\rho_{mg_{JJ}}}{\rho_{vg_{JJ}}}) \frac{S_L \Delta x_J}{\Delta \ell_{LJ}} + \frac{S^n_{cg_J}}{\Delta x_J}$$

Liquid Mass Equation

$$\frac{[(\alpha_\ell \rho_\ell)_J^n - (\alpha_\ell \rho_\ell)_J]}{\Delta t} A_{c_J} = \frac{\sum_{KB=1}^{NB} [(\alpha_\ell \rho_\ell)^* U_{\ell_{j-1}}^n A_{m_{j-1}}]_{KB} - \sum_{KA=1}^{NA} [(\alpha_\ell \rho_\ell)^* U_{\ell_j}^n A_{m_j}]_{KA}}{\Delta x_j}$$

$$+ \sum_{L=1}^{NKK} \gamma S_L [(\alpha_\ell \rho_\ell)^* V_{\ell_L}^n]_J - \frac{(1-\eta)\Gamma_J^n}{\Delta x_J} - \frac{S_J}{\Delta x_J} + \frac{S_{c\ell_J}^n}{\Delta x_J} \qquad (3)$$

Entrained Liquid Mass Equation

$$\frac{[(\alpha_e \rho_\ell)_J^n - (\alpha_e \rho_\ell)_J]}{\Delta t} A_{c_J} = \frac{\sum_{KB=1}^{NB} [(\alpha_e \rho_\ell)^* U_{e_{j-1}}^n A_{m_{j-1}}]_{KB} - \sum_{KA=1}^{NA} [(\alpha_e \rho_\ell)^* U_{e_j}^n A_{m_j}]_{KA}}{\Delta x_J}$$

$$+ \sum_{L=1}^{NKK} \gamma S_L [(\alpha_e \rho_\ell)^* V_{e_L}^n]_J - \frac{\eta \Gamma_J^n}{\Delta x_J} + \frac{S_J}{\Delta x_J} + \frac{S_{ce_J}^n}{\Delta x_J} \qquad (4)$$

Vapor Mass Equation

$$\frac{(\alpha_v\rho_v)_J^n - (\alpha_v\rho_v)_J}{\Delta t} A_{c_J} = \frac{\sum_{KB=1}^{NB} [(\alpha_v\rho_v)^* U^n_{vg_{j-1}} A_{m_{j-1}}]_{KB}}{\delta X_J}$$

$$- \frac{\sum_{KA=1}^{NA} [(\alpha_v\rho_v)^* U^n_{vg_j} A_{m_j}]_{KA}}{\Delta x_J} + \sum_{L=1}^{NKK} \gamma S_L [(\alpha_v\rho_v)^* V^n_{vg}]_{LJ}$$

$$+ \sum_{KB=1}^{NB} [(\alpha\rho_{vg})_{j-1} \epsilon_{D_{j-1}} (\frac{\rho_{v_J}}{\rho_{vg_J}} - \frac{\rho_{v_{j-1}}}{\rho_{vg_{j-1}}}) \frac{A_{m_{j-1}}}{\Delta x_{j-1}}]_{KB} \qquad (5)$$

$$- \sum_{KA=1}^{NA} (\alpha\rho_{vg})_j \epsilon_{D_j} (\frac{\rho_{v_{J+1}}}{\rho_{vg_{J+1}}} - \frac{\rho_{v_J}}{\rho_{vg_J}}) \frac{A_{m_j}}{\Delta x_j}]_{KA}$$

$$- \sum_{L=1}^{NKK} \gamma(\alpha\rho)_{vg_{LJ}} \epsilon_{D_L} (\frac{\rho_{v_{II}}}{\rho vg_{II}} - \frac{\rho_{v_{JJ}}}{\rho vg_{JJ}}) \frac{S_L \Delta x_J}{\Delta \ell_{LJ}} + \frac{S_n}{\Delta x_J} + \frac{S^n_{cv_J}}{\Delta x_j}$$

Rate of change of mass		Mass efflux in the vertical direction
$A \frac{\partial}{\partial t} (\alpha_k \rho_k)$	$=$ $-$	$\frac{\partial \alpha_k \rho_k U_k}{\partial x} A$

Mass efflux in the transverse direction		Mass efflux due to turbulent diffusion		Rate of creation of vapor mass due to phase change		Mass source due to entrainment		Phase source term
$- \sum_L (\alpha_k \rho_k V_k)_L S_L$	$-$	$\Delta \cdot \alpha_k \rho_{vg} \epsilon_D \nabla W_k$ (3 terms)	$+$	Γ'_k	$+$	S'	$+$	S_c

The reader should refer to the nomenclature list for the definition of each of the variables. The mass efflux in the transverse direction is given as the net mass leaving the cell through all transverse connections to all of the faces. The total number of transverse connections to the cell is NKK. The mass efflux in the vertical direction is given as the net mass leaving the cell through all vertical connections to the top and bottom of the cell. The total number of connections to the top of the cell is NA and the number of connections to the bottom of the cell is NB.

The velocity in each of the convection terms is taken to be the new time value while the convected quantity, in this case $(\alpha_k \rho_k)^*$, is taken at the old time. The turbulent diffusion terms are all calculated at the old time. The mass creation term is evaluated at the new time. However, it consists of an implicit and explicit part. The rate of mass generation due to phase change, Γ_J, is given by

$$\Gamma_J^n = \Gamma_{SHV} + \Gamma_{SHL} + \Gamma_{SCV} + \Gamma_{SCL} \tag{6}$$

where

$$\Gamma_{SHV} = \frac{HA_{SHV}\ (h_v - h_g)^n}{Cp_v\ (h_g - h_\ell)}$$

$$\Gamma_{SHL} = \frac{HA_{SHL}\ (h_\ell - h_f)^n}{Cp_\ell\ (h_g - h_\ell)}$$

$$\Gamma_{SCV} = \frac{HA_{SCV}\ (h_v - h_g)^n}{Cp_v\ (h_v - h_f)}$$

$$\Gamma_{SCL} = \frac{HA_{SCL}\ (h_\ell - h_f)^n}{Cp_\ell\ (h_v - h_f)}$$

The product of the interfacial area and heat transfer coefficient, the specific heats, and the heat of vaporization are all evaluated at the old time value and form the explicit portion of the mass creation term, while the enthalpies are evaluated at the new time value forming the implicit portion. This term is also multiplied by the ratio $(1-\alpha_v^n)/(1-\alpha_v)$ for vaporization or α_v^n/α_v for condensation. This is done to provide an implicit ramp that will cause the interfacial area to go to zero as all of the donor phase is depleted. An explicit ramp is also applied to the product (HA) to cause it to go to zero as the volume fraction of the donor phase approaches zero. The entrainment rate, S, is explicit and is also multiplied by implicit and explicit ramps that force it to zero as the donor liquid phase is depleted.

The last term in the equations is the phase mass source term, and it is evaluated at the new time. This term accounts for sources of phase mass that are exterior to the vessel mesh. These sources include mass sources due to chemical reaction, mass injection boundary conditions, and pressure boundary conditions. These source terms will be defined in the Section 3.0.

2.2.2 Fluid Energy Equations

Vapor Energy Equation

$$(\rho h)_{vg} = \rho_v h_v + \rho_{mg} h_{mg}$$

$$\frac{\{[\alpha_v(\rho h)_{vg}]_j^n - [\alpha_v(\rho h)_{vg}]_J\}A_{c_J}}{\Delta t} = \tag{7}$$

$$\frac{\sum_{KB=1}^{NB} \{[\alpha_v(\rho h)_{vg}]^* U^n_{vg_{j-1}} A_{m_{J-1}}]_{KB} - \sum_{KA=1}^{NA} \{[\alpha_v(\rho h)_{vg}]^* U^n_{vg_j} A_{m_j}]\}_{KA}}{\Delta x_J}$$

$$+ \sum_{L=1}^{NKK} \gamma S_L \{[\alpha_v(\rho h)_{vg}]^* V^n_{vg_{LJ}}]\}_J + \frac{\gamma^n_{ev_J}}{\Delta x_J} + \frac{q^n_{iv}}{\Delta x_J} + \frac{Q_{v_J}}{\Delta x_J} + \frac{S^n_{ev}}{\Delta x_J} + \frac{\alpha_{v_J}(P^n - P)_J A_{c_J}}{\Delta t}$$

where

$$\Gamma^n_{ev} = \Gamma_{SHV}\, h^n_g + \Gamma_{SCV}\, h^n_v + \Gamma_{SHL}\, h^n_g + \Gamma_{SCL}\, h^n_v$$

Liquid Energy Equation

$$\frac{\{[(\alpha_\ell + \alpha_e)\rho_\ell h_\ell]_J^n - [(\alpha_e + \alpha_\ell)\rho_\ell h_\ell]_J\}A_{c_J}}{\Delta t} =$$

$$\frac{1}{\Delta x_J}\{\sum_{KB=1}^{NB}\{(\alpha_\ell\rho_\ell h_\ell)^* U^n_{\ell_{j-1}} A_{m_{j-1}} + (\alpha_e\rho_\ell h_\ell)^* U^n_{e_{j-1}} A_{m_j}]_{KB} - \sum_{KA=1}^{NA}[(\alpha_\ell\rho_\ell h_\ell)^* U^n_{\ell_j} A_{m_j}$$

$$+ (\alpha_e\rho_\ell h_\ell)^* U^n_{e_j} A_{m_j}]_{KA}\} + \sum_{L=1}^{NKK}\gamma S_L\,[(\alpha_\ell\rho_\ell h_\ell)^* V^n_{\ell_L} + (\alpha_e\rho_\ell h_\ell)^* V^n_{e_L}]_J$$

$$- \frac{\Gamma^n_{e\ell}}{\Delta x_j} + \frac{q^n_{i\ell_J}}{\Delta x_J} + \frac{Q_{\ell_J}}{\Delta x_J} + \frac{S^n_{e\ell}}{\Delta x_J} + \frac{Q^T_{\ell_J}}{\Delta x_J} + \frac{\alpha_{\ell_J}(p^n - P)_J A_{c_J}}{\Delta t} \qquad (8)$$

where

$$\Gamma^n_{e\ell} = -\Gamma_{SHV}h_\ell - \Gamma_{SCV}h_f - \Gamma_{SHL}h_\ell - \Gamma_{SCL}h_f$$

Rate of change of enthalpy		Efflux of enthalpy in the vertical direction
$A \frac{\partial}{\partial t} (\alpha_k \rho_k h_k)$	$= -$	$\frac{\partial}{\partial x} (\alpha_k \rho_k h_k U_k)$

$$- \left[\text{Efflux of enthalpy in the transverse direction} \right] + \left[\text{Energy source due to mass transfer between fields} \right]$$

$$- \left[\sum_L (\alpha_k \rho_k h_k V_k)_L \, S_L \right] + \left[\Gamma_{ek} \right]$$

$$+ \left[\text{Interfacial heat transfer} \right] + \left[\text{Heat addition from solid} \right] + \left[\text{Fluid conduction and turbulent heat flux} \right] + \left[\text{Work term} \right]$$

$$+ \left[q' \right] + \left[Q' \right] + \left[\nabla \cdot [\alpha_k (\underline{q}_k + \underline{q}_k)^T] \right] + \left[\alpha \frac{\partial P}{\partial t} \right]$$

Again, the energy efflux in the transverse direction is the sum of all transverse connections on all faces of the cell; that in the vertical direction is the sum of all connections to the top and bottom of the cell. New time velocities convect the donor cell $(\alpha_k \rho_k h_k)^*$, which is evaluated using old time values. New time enthalpies are convected in the phase change term. The interfacial heat transfer term, like the vapor generation term, has an implicit temperature difference and an explicit heat transfer coefficient and interfacial area. The wall heat transfer is explicit. The energy source terms corresponding to the mass source terms will be defined in Section 3.0. The fluid conduction and turbulent heat flux are explicit and will be expanded in Section 3.0.

2.2.3 Momentum Equations in the Vertical Direction

Vapor Phase

$$\rho_{vg} = \rho_v + \rho_g$$

$$\frac{[(\alpha_v \rho_{vg} U_{vg})_j^n - (\alpha_v \rho_{vg} U_{vg})_j] A_{m_j}}{\Delta t} = \sum_{KB=1}^{NB} \frac{[(\alpha_v \rho_{vg} U_{vg})^* U_{vg_J}]_{KB} A_{m_{KB}}}{\Delta x_j}$$

$$- \sum_{KA=1}^{NA} \frac{[(\alpha_v \rho_{vg} U_{vg})^* U_{vg}{}_{J+1}]_{KA} A_{m}{}_{KA}}{\Delta x_j} + \sum_{LB=1}^{NKB} \gamma[(\alpha_v \rho_{vg} U_{vg})^* V_{vg_J}]_{LB} \frac{S_{LB}}{2} \qquad (9)$$

$$+ \sum_{LA=1}^{NKA} \gamma[(\alpha_v \rho_{vg} U_{vg})^* V_{vg_{J+1}}]_{LA} \frac{S_{LA}}{2} - (\alpha_v \rho_{vg})_j \, g \, A_{m_j} - \frac{(P_{J+1} - P_J)^n}{\Delta x_j} \alpha_{v_j} A_{m_j}$$

$$- K_{v_j} (2U_{vg_j}^n - U_{vg_j}) A_{m_j} - K_{v\ell_j} [2(U_{vg} - U_\ell)_j^n - (U_{vg} - U_\ell)_j] A_{m_j}$$

$$- K_{ve_j} [2(U_{vg} - U_e)_j^n - (U_{vg} - U_e)_j] A_{m_j}$$

$$- \frac{[\Gamma_C U_{vg} - (1-\eta)\Gamma_E U_\ell - \eta \Gamma_E U_e]_j}{\Delta x_j} + \frac{S_{mv_j}}{\Delta x_j} + T_{v_j}^T$$

Liquid Phase

$$\frac{[(\alpha_\ell \rho_\ell U_\ell)_j^n - (\alpha_\ell \rho_\ell U_\ell) A_{m_j}}{\Delta t} = \frac{\sum_{KB=1}^{NB} [(\alpha_\ell \rho_\ell U_\ell)^* U_{\ell_J}]_{KB} A_{m_{KB}}}{\Delta x_j}$$

$$- \frac{\sum_{KA=1}^{NA} [(\alpha_\ell \rho_\ell U_\ell)^* U_{\ell_{J+1}}]_{KA} A_{m_{KA}}}{\Delta x_j} + \sum_{LB=1}^{NKB} \gamma [(\alpha_\ell \rho_\ell U_\ell)^* V_{\ell_J}]_{LB} \frac{S_{LB}}{2} \qquad (10)$$

$$+ \sum_{LA=1}^{NKA} \gamma [(\alpha_\ell \rho_\ell U_\ell)^* V_{\ell_{J+1}}]_{LA} \frac{S_{LA}}{2} - (\alpha_\ell \rho_\ell)_j \, g \, A_{m_j}$$

$$- \frac{(P_{J+1} - P_J)^n}{\Delta x_j} \alpha_{\ell_j} A_{m_j}$$

$$- K_{\ell_j} (2U_{\ell_j}^n - U_{\ell_j}) A_{m_j} + K_{v\ell_j} [2(U_v - U_\ell)_j^n - (U_v - U_\ell)_j] A_{m_j}$$

$$+ \frac{(1-\eta) [\Gamma_C U_v - \Gamma_E U_\ell]_j}{\Delta x_j}$$

$$+ \frac{(S_D U_e - S_E U_\ell)_j}{\Delta x_j} + \frac{S_{m\ell_j}}{\Delta x_j} + T_{\ell_j}^T$$

Entrained Liquid Phase

$$\frac{[(\alpha_e \rho_\ell U_e)_j^n - (\alpha_e \rho_\ell U_e)_j] A_{m_j}}{\Delta t} = \frac{\sum_{KB=1}^{NB} [(\alpha_e \rho_\ell U_e)^* U_{e_J}]_{KB} A_{m_{KB}}}{\Delta x_j}$$

$$- \frac{\sum_{KA=1}^{NA} [(\alpha_e \rho_\ell U_e)^* U_{e_{j+1}}]_{KA} A_{m_{KA}}}{\Delta x_j} + \sum_{LB=1}^{NKB} \gamma [(\alpha_e \rho_\ell U_e)^* V_{e_J}]_{LB} \frac{S_{LB}}{2}$$

(11)

$$+ \sum_{LA=1}^{NKA} \gamma [(\alpha_e \rho_\ell U_e)^* V_{e_{J+1}}]_{LA} \frac{S_{LA}}{2} - (\alpha_e \rho_\ell)_j \, g \, A_{m_j}$$

$$- \frac{(P_{J+1} - P_J)^n}{\Delta x_j} \alpha_{e_j} A_{m_j}$$

$$- K_{e_j} (2U_{e_j}^n - U_{e_j}) A_{m_j} + K_{ve_j} [2(U_v - U_e)_j^n - (U_v - U_e)_j] A_{m_j} + \frac{\eta [\Gamma_C U_v - \Gamma_E U_e]_j}{\Delta x_j}$$

$$- \frac{(S_D U_e - S_E U_\ell)_j}{\Delta x_j} + \frac{S_{me_j}}{\Delta x_j}$$

$$\left[\begin{array}{l}\text{Rate of change}\\ \text{of vertical}\\ \text{momentum}\\ \\ A\,\dfrac{\partial(\alpha_k\rho_k U_k)}{\partial t}\end{array}\right] = -\left[\begin{array}{l}\text{Efflux of momentum in}\\ \text{the axial direction}\\ \\ A\,\dfrac{\partial}{\partial x}\,(\alpha_k\rho_k U_k U_k)\end{array}\right]$$

$$-\left[\begin{array}{l}\text{Efflux of momentum in}\\ \text{the transverse direction}\\ \\ \sum_L\,(\alpha_k\rho_k U_k V_k)_L\,S_L\end{array}\right] - \left[\begin{array}{l}\text{Gravitational}\\ \text{force}\\ \\ \alpha_k\rho_k g\end{array}\right]$$

$$\left[\begin{array}{l}\text{Pressure gradient}\\ \\ \alpha_k\,\dfrac{\partial P}{\partial x}\end{array}\right] - \left[\begin{array}{l}\text{Wall shear}\\ \\ \tau_w\end{array}\right] + \left[\begin{array}{l}\text{Interfacial shear}\\ \\ \tau_{i_{v\ell}} + \tau_{i_{ve}}\end{array}\right]$$

$$\left[\begin{array}{l}\text{Momentum source due}\\ \text{to mass transfer}\\ \text{between phases}\\ \\ \Gamma U + SU\end{array}\right] + \left[\begin{array}{l}\text{Momentum source term}\\ \\ S_m\end{array}\right] + \left[\begin{array}{l}\text{Viscous and turbulent}\\ \text{shear stress}\\ \\ \nabla \cdot [\alpha_k(\underline{\underline{\sigma}}_k + \underline{\underline{I}}_k^T)]\end{array}\right]$$

The momentum efflux in the vertical direction is given as the net momentum leaving the cell through all vertical connections. The total number of momentum mesh cells facing the top of the cell is NA and the total facing the bottom of the cell is NB. The momentum efflux in the transverse direction is given as the net momentum leaving the cell through all transverse connections. The total number of transverse connections to the top half of the momentum cell is NKA. The total number of connections to the bottom half of the cell is NKB. To achieve stability with this semi-implicit formulation of the momentum equation, donor cell momentum, $(\alpha_k\rho_k U_k)^*$, is convected by the velocities at the momentum cell face. A simple linear average between adjacent momentum cell velocities is taken to obtain the velocity at momentum cell faces:

$$U_J = \frac{U_j + U_{j-1}}{2} \tag{12}$$

Likewise, linear averages are used to obtain other variables at locations where they are not defined. The void fraction of the momentum cell is given as

$$\alpha_j = \frac{\alpha_J + \alpha_{J+1}}{2} \tag{13}$$

and the density is given as

$$\rho_j = \frac{\rho_J + \rho_{J+1}}{2} \tag{14}$$

The momentum equations are solved for the phase flows ($\alpha_k \rho_k U_k A_m$). Velocities are obtained from the flow by dividing it by the momentum cell density and momentum cell area:

$$U_{k_j} = \frac{(\alpha_k \rho_k U_k A_m)_j}{(\alpha_k \rho_k A_m)_j} \tag{15}$$

The pressures in the pressure force term are taken at the new time, as are the velocities in the wall shear and interfacial shear terms. The shear terms have been weighted toward the new time velocity by differencing them in the form $K(2U^n - U)$. All other terms and variables are computed using old time values. The donor phase momentum is convected during mass exchange between fields. The explicit viscous and turbulent shear stresses will be expanded in Section 3.0.

2.2.4 Momentum Equations in the Transverse Directions

Vapor Phase

$$\frac{[(\alpha_v\rho_{vg}V_{vg})^n - (\alpha_v\rho_{vg}V_{vg})]_J\, S_J\Delta x_J}{\Delta t} = \frac{\sum_{L=1}^{NKII} \gamma[(\alpha_v\rho_{vg}V_{vg})^*_J\, V_{vg_L}\, S_L]\Delta x_J}{\Delta \ell_J}$$

$$- \frac{\sum_{L=1}^{NKJJ} \gamma[\alpha_v \rho_{vg} V_{vg})^*_J\, V_{vg_L}\, S_L]\Delta x_J}{\Delta \ell_J} + \frac{\sum_{L=1}^{NG} \gamma[(\alpha_v \rho_{vg} V_{vg})^*_J\, W_{vg_L}\, \frac{S_L}{2}]\, \Delta x_J}{\Delta \ell_J}$$

$$+ \frac{\sum_{IB=1}^{NCB} [(\alpha_v\rho_{vg}V_{vg})^*\, U_{vg_{IB}}\, ALAT_{IB}]}{\Delta \ell_J} - \frac{\sum_{IA=1}^{NCA} [(\alpha_v\rho_{vg}V_{vg})^*\, U_{vg_{IA}}\, ALAT_{IA}]}{\Delta \ell_J} \qquad (16)$$

$$- \frac{\alpha_{v_{II-JJ}}\, (P_{JJ} - P_{II})^n\, S_J\Delta x_J}{\Delta \ell_J} - K_{v_J}\, (2V^n_{vg_J} - V_{vg_J})\, S_J\Delta x_J - K_{v\ell_J}[2(V_{vg} - V_\ell)^n_J$$

$$- (V_{vg} - V_\ell)_J]S_J\Delta x_J$$

$$- K_{ve_J}[2(V_{vg} - V^n_e)_J - (V_{vg} - V_e)_J]S_J\Delta x_J - \frac{[\Gamma_C V_{vg} - (1 - \eta)\Gamma_E V_\ell - \eta\Gamma_E V_e]_J}{\Delta x_J}$$

$$+ \frac{S_{mv_J}}{\Delta \ell_J} + T^T_{v_J}$$

Liquid Phase

$$\frac{[(\alpha_\ell \rho_\ell V_\ell)^n - (\alpha_\ell \rho_\ell V_\ell)]_J \, S_J \Delta x_J}{\Delta t} = \frac{\sum_{L=1}^{NKII} \gamma[(\alpha_\ell \rho_\ell V_\ell)_J^* \, V_{\ell_L} \, S_L] \Delta x_J}{\ell_J}$$

$$- \frac{\sum_{L=1}^{NKJJ} \gamma[(\alpha_\ell \rho_\ell V_\ell)_J^* \, V_{\ell_L} \, S_L] \Delta x_J}{\Delta \ell_J} + \frac{\sum_{L=1}^{NG} \gamma[(\alpha_\ell \rho_\ell V_\ell)_J^* \, W_{\ell_L} \, \frac{S_L}{2}] \Delta x_J}{\Delta \ell_J}$$

$$+ \frac{\sum_{IB=1}^{NCB} [(\alpha_\ell \rho_\ell V_\ell)^* \, U_{\ell_{IB}} \, ALAT_{IB}]}{\Delta \ell_J} - \frac{\sum_{IA=1}^{NCA} [(\alpha_\ell \rho_\ell V_\ell)^* \, U_{\ell_{IA}} \, ALAT_{IA}]}{\Delta \ell_J} \qquad (17)$$

$$- \frac{\alpha_{\ell_{II-JJ}} \, (P_{JJ} - P_{II})^n \, S_J \Delta x_J}{\Delta \ell_J} - K_{\ell_J} \, (2V_{\ell_J}^n - V_{\ell_J}) \, S_J \Delta x_J$$

$$+ K_{v\ell_j} \, [2(V_v - V_\ell)_J^n - (V_v - V_\ell)_J] S_j \Delta x_j$$

$$+ \frac{[(1-\eta)\Gamma_C V_v - (1-\eta)\Gamma_E V_\ell]_J}{\Delta \ell_J} + \frac{S_{m\ell_J}}{\Delta \ell_J} + T_{\ell_J}^T + \frac{(S_D V_e - S_E V_e)_J}{\Delta \ell_J}$$

Entrained Liquid Phase

$$\frac{(\alpha_e\rho_\ell V_e)^n - (\alpha_e\rho_\ell V_e)]_J S_J\Delta x_J}{\Delta t} = \frac{\sum_{L=1}^{NKII} \gamma[(\alpha_2\rho_\ell V_e)_J^* V_{e_L} S_L]\Delta x_J}{\Delta\ell_J}$$

$$- \frac{\sum_{L=1}^{NKJJ} \gamma[(\alpha_e\rho_\ell V_e)_J^* V_{e_L} S_L]\Delta x_J}{\Delta\ell_J} + \frac{\sum_{L=1}^{NG} \gamma[(\alpha_e\rho_\ell V_e)_J^* W_{e_L} \frac{S_L}{2}]\Delta x_J}{\Delta\ell_J}$$

$$+ \frac{\sum_{IB=1}^{NCB} [(\alpha_e\rho_\ell V_e)^* U_{e_{IB}} ALAT_{IB}]}{\Delta\ell_J} - \frac{\sum_{IA=1}^{NCA} [(\alpha_e\rho_\ell V_e)^* U_{e_{IA}} ALAT_{IA}]}{\Delta\ell_J} \qquad (18)$$

$$- \frac{\alpha_{e_{II-JJ}} (P_{JJ} - P_{II})^n S_J\Delta x_J}{\Delta\ell_J} - K_{e_J} (2V_{e_J}^n - V_{e_J}) S_J Dx_J$$

$$+ K_{ve_j} [2(V_{vg} - V_e)_j^n - (V_{vg} - V_e)_j] S_J\Delta x_J$$

$$+ \frac{(\eta\Gamma_C V_v - \eta\Gamma_E V_e)_J}{\Delta\ell_J} + \frac{S_{me_J}}{\Delta\ell_J} - \frac{(S_D V_e - S_e V_e)_J}{\Delta\ell_J}$$

$$\left[\begin{array}{l}\text{Rate of change}\\ \text{of transverse}\\ \text{momentum}\\ \\ A\,\dfrac{\partial(\alpha_k\rho_k V_k)}{\partial t}\end{array}\right] = -\left[\begin{array}{l}\text{Transverse}\\ \text{momentum efflux}\\ \text{by transverse convection}\\ \\ \dfrac{\partial(\alpha_k\rho_k V_k V_k A)}{\partial L}\end{array}\right] - \left[\begin{array}{l}\text{Transverse}\\ \text{momentum efflux}\\ \text{by orthogonal}\\ \text{transverse convection}\\ \\ \sum\limits_{NK}(\alpha_k\rho_k V_k V_{k_{NK}})S_{NK}\end{array}\right]$$

$$+\left[\begin{array}{l}\text{Transverse}\\ \text{momentum efflux}\\ \text{by vertical convection}\\ \\ \dfrac{\partial}{\partial x}\,\alpha_k\rho_k V_k U_k A\end{array}\right] - \left[\begin{array}{l}\text{Pressure gradient}\\ \text{force}\\ \\ \alpha_k A\,\dfrac{\partial P}{\partial T}\end{array}\right] - \left[\begin{array}{l}\text{Transverse}\\ \text{wall shear}\\ \\ \tau_{wk}\,A\end{array}\right]$$

$$+\left[\begin{array}{l}\text{Interfacial drag}\\ \text{between vapor}\\ \text{and continuous}\\ \text{liquid}\\ \\ \tau_{i_{\ell v}}\,A\end{array}\right] + \left[\begin{array}{l}\text{Interfacial drag}\\ \text{between vapor}\\ \text{and drops}\\ \\ \tau_{i_{ev}}\,A\end{array}\right]$$

$$+\left[\begin{array}{l}\text{Transverse momentum}\\ \text{source due to mass}\\ \text{transfer between}\\ \text{phases}\\ \\ \Gamma H + SV\end{array}\right] + \left[\begin{array}{l}\text{Transverse momentum}\\ \text{source term}\\ \\ S_m\end{array}\right] + \left[\begin{array}{l}\text{Viscous and turbulent}\\ \text{shear stress}\\ \\ \nabla \cdot [\alpha_k\,(\underline{\sigma}_k + \underline{T}_k^T)]\end{array}\right]$$

As in the vertical momentum equations, the pressures in the pressure force term and the velocities in the wall and interfacial drag term are the new time values, while all other terms and variables are computed using old time values. The momentum efflux by transverse convection is given as the sum of the momentum entering (or leaving) the cell through all transverse connections. Momentum convected by transverse velocities (that are in the direction of the transverse

velocity being solved for) is the sum of the momentum entering (or leaving) through mesh cell faces connected to the face of the mesh cell for which the momentum equation is being solved. NKII is the number of mesh cells facing the upstream face of the mesh cell, and NKJJ is the number facing the downstream face of the mesh cell. Momentum convected out the sides of the mesh cell by velocities that are orthogonal to the velocity to be solved for is given by the sum of the momentum convected into (or out of) cells connected to the sides of the transverse momentum mesh cell. The number of cells connected to the mesh cell under consideration, whose velocities are orthogonal to its velocity, is given by NG. The momentum convected through the top and bottom of the mesh cell by vertical velocities is the sum of the momentum convected into (or out of) cells connected to the top and bottom of the mesh cell and depends on the number of cells connected to the top (NCA) and bottom (NCB) of the mesh cell.

A simple linear average is used to obtain velocities at mesh cell faces:

$$V_{L_{II}} = \frac{V_{J_{LL}} + V_J}{2} \tag{19}$$

Linear averages also are used to obtain other variables at locations where they are not defined. Velocities are obtained from the flows by dividing by the momentum cell density and transverse momentum flow area:

$$V_{k_J} = \frac{(\alpha_k \rho_k V_k S \Delta x)_J}{(\alpha_k \rho_k S \Delta x)_J} \tag{20}$$

Donor cell differencing is used for all convective terms, and the donor phase momentum is convected in the mass transfer terms.

3.0 SOURCE, VISCOUS, AND TURBULENCE TERMS

Terms not fully expanded in the presentation of the finite-volume equations in Section 2.0 are presented in this section. These include the mass, energy, and momentum source terms; the viscous shear stress tensors; the turbulent shear stress tensors; the fluid conduction vector; and the turbulent heat flux vector.

3.1 Mass, Energy, and Momentum Source Terms

Source terms are required for the mass, energy, and momentum finite-volume equations to account for the arbitrary boundary conditions that may be specified anywhere in the mesh.

Five basic types of boundary conditions may be specified within the mesh. The first type allows the user to specify the pressure and the mixture enthalpy in any cell. The normal momentum equations are then solved on the cell faces to obtain flows into or out of the cell. Properties specified within the cell are convected to surrounding cells if the flow is out of the cell. Properties of surrounding cells are convected into the specified cell if the flow is into the cell. However, because the properties of the cell are specified, the pressure, temperature, and void fractions do not change accordingly, so the pressure boundary condition can act as a mass, energy, and momentum sink if flow is into the cell, or as a source if flow is out of the cell.

The second type of boundary condition allows the user to specify the mixture enthalpy, and pressure within the cell and the continuity mass flow rate at the top of the cell. All three phases are assumed to have the same velocity at the cell face. No momentum solution is performed at the top of the cell for this case because the flow is specified. Otherwise, the boundary condition behaves in the same way as the first type of boundary condition, acting as a source (or sink) of mass, momentum, and energy, depending on the direction of flow.

The third type of boundary condition sets the flow on any mesh cell face, and therefore does not produce any mass, momentum, or energy sources.

The fourth type of boundary condition allows the user to specify a mass and energy source in any computational cell without changing the computed fluid properties within the cell. Again, all three phases are assumed to travel at the mixture velocity, and the amount of flow is determined by the volume fraction of each phase specified in the boundary condition. Momentum of this source is added only if the flow is in the transverse direction and into the mesh, or if flow is out of the mesh.

The final type of boundary condition allows the user to specify a pressure sink to be connected to any cell. A simple momentum equation is solved between the sink pressure and the cell pressure, and the resulting flow produces a mass,

momentum, and energy sink if flow is out of the mesh and a mass and energy source if the flow is into the mesh. The sink vapor momentum equation is

$$(\alpha_v \rho_v V_v A)^n_{SINK} = (\alpha_v \rho_v V_v A) + \frac{\Delta t}{\Delta X}_{SINK} A_{SINK} (P_{SINK} - P_J) \qquad (21)$$

$$- K_{v_{SINK}} U^n_{v_{SINK}} A_{SINK} - k_{v\ell} (U_v - U_\ell)^n_{SINK} A_{SINK} - K_{ve} (U_v - U_e)^n_{SINK} A_{SINK}$$

The energy and mass source terms for pressure boundary conditions use semi-implicit velocities. All other boundary condition source terms are explicit. Donor cell differences are used for all source terms. The donor cell is determined by the sign of the boundary condition velocity. If flow is out of the mesh, then mesh cell properties are used. If flow is entering the mesh, then the specified boundary condition properties are used.

3.2 Viscous and Turbulent Shear Stress Tensors and Heat Flux Vectors

The viscous and turbulent shear stress represented in the finite-volume equation given in Section 2.0 by $T^T_{k_j}$ are expanded in this section. This term represents a particular component of the viscous and turbulent stress tensors, $E \cdot [\alpha_k(\underline{\underline{\sigma}}_k + \underline{\underline{T}}^T_k)]$. The viscous stress tensor may be written as

$$\underline{\underline{\sigma}}_k = \begin{bmatrix} \sigma_{k_{xx}} & \sigma_{k_{xy}} & \sigma_{k_{xz}} \\ \sigma_{k_{yx}} & \sigma_{k_{yy}} & \sigma_{k_{yz}} \\ \sigma_{k_{zx}} & \sigma_{k_{zy}} & \sigma_{k_{zz}} \end{bmatrix} \qquad (22)$$

The turbulent stress tensor $\underline{\underline{T}}^T_k$ may be written in a similar way. Further,

$$\nabla \cdot [\alpha_k (\underline{g}_k + \underline{\underline{I}}_k^T)] \{\frac{\partial}{\partial x} [\alpha_k (\sigma_{k_{xx}} + T_{k_{xx}}^T)] + \frac{\partial}{\partial y} [\alpha_k (\sigma_{k_{yx}} + T_{k_{yx}}^T)]$$

$$+ \frac{\partial}{\partial z} [\alpha_k (\sigma_{k_{zx}} + T_{k_{zx}}^T)]\} \underline{i} + \{\frac{\partial}{\partial x} [\alpha_k (\sigma_{k_{xy}} + T_{k_{xy}}^T)] \quad (23)$$

$$+ \frac{\partial}{\partial y} [\alpha_k (\sigma_{k_{yy}} + T_{k_{yy}}^T)] + \frac{\partial}{\partial z} [\alpha_k (\sigma_{k_{zy}} + T_{k_{zy}}^T)]\} \underline{j}$$

$$+ \{\frac{\partial}{\partial x} [\alpha_k (\sigma_{k_{xz}} + T_{k_{xz}}^T)] + \frac{\partial}{\partial y} [\alpha_k (\sigma_{k_{yz}} + T_{k_{yz}}^T)] + \frac{\partial}{\partial z} [\alpha_k (\alpha_{k_{zz}} + Tk_{zz}^T)]\} \underline{k}$$

The coordinate system used is shown in Figure 5.

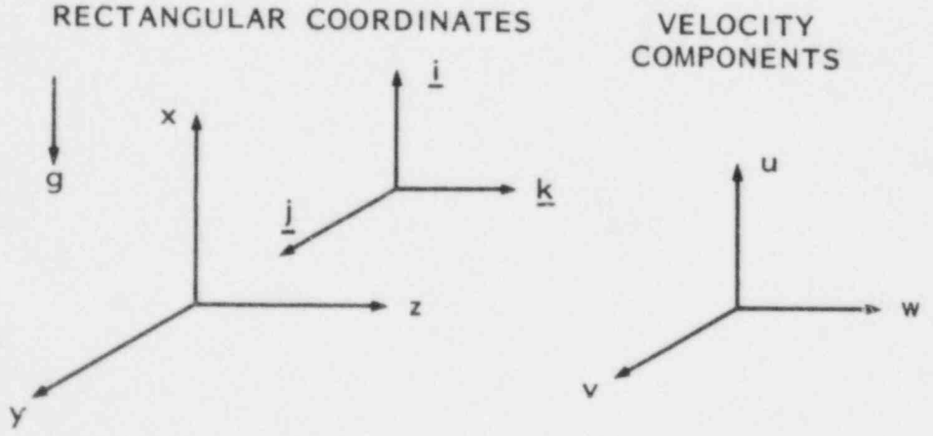

Figure 5 Coordinate system and nomenclature

The first subscript on the shear stress denotes the face on which the stress is acting; the second subscript denotes the direction in which the stress acts. (For example, $\sigma_{k_{ij}}$ is the shear stress acting on face i in the j direction.)

The viscous and turbulent stresses are defined in terms of the bulk deformation tensor, $\underline{\underline{D}}_{k_B}$, given by

$$\underline{\underline{D}}_{k_B} = \frac{1}{2} [\nabla u + (\nabla u)^t] \tag{24}$$

or

$$\underline{\underline{D}}_{k_B} = \begin{bmatrix} \frac{\partial u}{\partial x} & \frac{1}{2}\left(\frac{\partial u}{\partial y} + \frac{\partial v}{\partial x}\right) & \frac{1}{2}\left(\frac{\partial u}{\partial z} + \frac{\partial w}{\partial x}\right) \\ \frac{1}{2}\left(\frac{\partial u}{\partial y} + \frac{\partial v}{\partial x}\right) & \frac{\partial v}{\partial y} & \frac{1}{2}\left(\frac{\partial v}{\partial z} + \frac{\partial w}{\partial y}\right) \\ \frac{1}{2}\left(\frac{\partial u}{\partial z} + \frac{\partial w}{\partial x}\right) & \frac{1}{2}\left(\frac{\partial v}{\partial z} + \frac{\partial w}{\partial y}\right) & \frac{\partial w}{\partial z} \end{bmatrix} \tag{25}$$

Eliminating the normal stresses such that the diagonal term is zero gives the deleted bulk deformation tensor $\underline{\underline{D}}^*_{k_B}$.

Neglecting the viscous contribution to the normal stresses and eliminating the normal stress due to pressure already accounted for in the finite-difference equation leaves

$$\underline{\underline{\sigma}}_k = 2\mu \underline{\underline{D}}^*_{k_B} \tag{26}$$

or

$$\sigma_{k_{xy}} = \sigma_{k_{yx}} = \mu\left(\frac{\partial u}{\partial y} + \frac{\partial v}{\partial x}\right) \tag{27}$$

$$\sigma_{k_{xz}} = \sigma_{k_{zx}} = \mu\left(\frac{\partial u}{\partial z} + \frac{\partial w}{\partial x}\right) \tag{28}$$

$$\sigma_{k_{yz}} = \sigma_{k_{zy}} = \mu\left(\frac{\partial v}{\partial z} + \frac{\partial w}{\partial y}\right) \tag{29}$$

The turbulent stress tensor is given by

$$\underline{\underline{T}}^T_k = - P^T_k \underline{\underline{F}}_k + 2\, \mu^T_k \underline{\underline{D}}^*_{k_B} \tag{30}$$

P^T is the turbulent pressure, $\underline{\underline{F}}$ is the anisotropy tensor, which is generally assumed to be equal to the unit tensor, and μ^T is the turbulent or "eddy" viscosity. The turbulent stress tensor may be written in matrix form as

$$\underline{\underline{T}}^T_k = \begin{bmatrix} -P^T_k F_{k_{xx}} & \mu^T_k \left(\frac{\partial u}{\partial y} + \frac{\partial v}{\partial x}\right) & \mu^T_k \left(\frac{\partial u}{\partial z} + \frac{\partial w}{\partial x}\right) \\ \mu^T_k \left(\frac{\partial u}{\partial y} + \frac{\partial w}{\partial x}\right) & - P^T_k F_{k_{yy}} & \mu^T_k \left(\frac{\partial v}{\partial z} + \frac{\partial w}{\partial y}\right) \\ \mu^T_k \left(\frac{\partial u}{\partial z} + \frac{\partial w}{\partial x}\right) & \mu^T_k \left(\frac{\partial v}{\partial z} + \frac{\partial w}{\partial y}\right) & - P^T_k F_{k_{zz}} \end{bmatrix} \tag{31}$$

The turbulent viscosity is given by

$$\mu^T_k = \rho_k \ell^2_m \sqrt{2\underline{\underline{D}}^*_{k_B} : \underline{\underline{D}}^*_{k_B}} \tag{32}$$

and the turbulent pressure by

$$P^T_k = \rho_k \ell^2_m \left(2\, \underline{\underline{D}}^*_{k_B} : \underline{\underline{D}}^*_{k_B}\right) \tag{33}$$

The double dot indicates a second-order tensor inner product resulting in a scalar quantity. Here this gives

$$2\,\underline{\underline{D}}^{*}_{k_B} : \underline{\underline{D}}^{*}_{k_B} = \left(\frac{\partial u}{\partial y} + \frac{\partial v}{\partial x}\right)^2 + \left(\frac{\partial u}{\partial z} + \frac{\partial w}{\partial x}\right)^2 + \left(\frac{\partial v}{\partial z} + \frac{\partial w}{\partial y}\right)^2 \tag{34}$$

Now that all of the terms for the viscous and turbulent shear stresses have been expanded, the finite-difference form of the terms can be presented. The total force resulting from viscous and turbulent shear stresses acting on a mesh cell may be obtained using the divergence theorem:

$$E = \iiint_{vol} \nabla \cdot [\alpha_k \, (\underline{\underline{\sigma}}_k + \underline{\underline{T}}^{T}_{k})]dv = \iint_{surface} n \cdot [\alpha_k (\underline{\underline{\sigma}}_k + \underline{\underline{T}}^{T}_{k})]ds \tag{35}$$

The finite-difference approximation for this total force is

$$\begin{aligned}
\underline{F} = \underline{i} \cdot \{ & \alpha_k(\sigma_{k_{xx}} + T^T_{k_{xx}})|_{+x}\Delta y\Delta z - \alpha_k(\sigma_{k_{xx}} + T^T_{k_{xx}} + T^T_{k_{xx}})|_{-x}\Delta y\Delta z \\
& + \alpha_k(\sigma_{k_{yx}} + T^T_{k_{yx}})|_{+y}\Delta x\Delta z - \alpha_k(\sigma_{k_{yx}} + T^T_{k_{yx}})|_{-y}\Delta x\Delta z \\
& + \alpha_k(\sigma_{k_{zx}} + T^T_{k_{zx}})|_{+z}\Delta x\Delta z - \alpha_k(\sigma_{k_{zx}} + T^T_{k_{zx}})|_{-z}\Delta x\Delta y\} \\
& + \underline{j} \cdot \{\alpha_k(\sigma_{k_{xy}} + T^T_{k_{xy}})|_{+x}\Delta y\Delta z - \alpha_k(\sigma_{k_{xy}} + T^T_{k_{xy}})|_{-x}\Delta y\Delta z \\
& + \alpha_k(\sigma_{k_{yy}} + T^T_{k_{yy}})|_{+y}\Delta x\Delta z - \alpha_k(\sigma_{k_{yy}} + T^T_{k_{yy}})|_{-y}\Delta x\Delta z \\
& + \alpha_k(\sigma_{k_{zy}} + T^T_{k_{zy}})|_{+z}\Delta x\Delta z - \alpha_k(\sigma_{k_{zy}} + T^T_{k_{zy}})|_{-z}\Delta x\Delta z\} \\
& + \underline{k} \cdot \{\alpha_k(\sigma_{k_{xz}} + T^T_{k_{xz}})|_{+x}\Delta y\Delta z - \alpha_k(\sigma_{k_{xz}} + T^T_{k_{xz}})|_{-x}\Delta y\Delta z \\
& + \alpha_k(\sigma_{k_{yz}} + T^T_{k_{yz}})|_{+y}\Delta x\Delta z - \alpha_k(\sigma_{k_{yz}} + T^T_{k_{yz}})|_{-y}\Delta x\Delta z \\
& + \alpha_k(\sigma_{k_{zz}} + T^T_{k_{zz}})|_{+z}\Delta x\Delta z - \alpha_k(\sigma_{k_{zz}} + T^T_{k_{zz}})|_{-z}\Delta x\Delta z \qquad (36)
\end{aligned}$$

The stresses ($\sigma_{k_{xx}}$, $\tau_{k_{xx}}$, $\sigma^{T}_{k_{yx}}$, $\tau^{T}_{k_{yx}}$, etc.) must be evaluated on various transverse momentum cells. For example, the stresses acting in the vertical direction on a vertical momentum cell are shown in Figure 6.

The velocity gradients are calculated by taking differences between adjacent cell velocities to obtain values for $\Delta u/\Delta z$ and $\Delta w/\Delta \ell$ on continuity cell edges. This is illustrated in Figure 7.

In Figure 7, the velocity gradient at point A is given by

$$\left(\frac{\partial u}{\partial z} + \frac{\partial w}{\partial x}\right)_A + \left(\frac{u_2 - u_1}{\Delta \ell} + \frac{w_2 - w_1}{\Delta x}\right) \tag{37}$$

The derivatives for the other edges are computed in a similar fashion and the process is repeated for other cells. If a solid surface bounds the cell in the transverse direction, it is assumed that the velocity gradient is zero at the wall. Velocity is assumed to be zero at the wall for solid surfaces that bound the cell in a vertical direction.

The derivative at the mass cell center is obtained by taking a four-point average of the derivatives on the cell edges:

$$\left(\frac{\partial u}{\partial z} + \frac{\partial w}{\partial x}\right)_{\text{cell center}} = \frac{1}{4}\left[\left(\frac{\partial u}{\partial z} + \frac{\partial w}{\partial x}\right)_A + \left(\frac{\partial u}{\partial z} + \frac{\partial w}{\partial x}\right)_B + \left(\frac{\partial u}{\partial z} + \frac{\partial w}{\partial x}\right)_C + \left(\frac{\partial u}{\partial z} + \frac{\partial w}{\partial x}\right)_D\right] \tag{38}$$

The same procedure is used to find $\left(\frac{\partial u}{\partial y} + \frac{\partial v}{\partial x}\right)$ and $\left(\frac{\partial v}{\partial z} + \frac{\partial w}{\partial x}\right)$ at the mass cell center. The quantity $2\underline{\underline{D}}^{*}_{k_B} : \underline{\underline{D}}^{*}_{k_B}$ at the cell center is calculated from Equation 34 using these averaged derivatives. The turbulent viscosity and turbulent pressure are then calculated at the cell center using Equations 32 and 33.

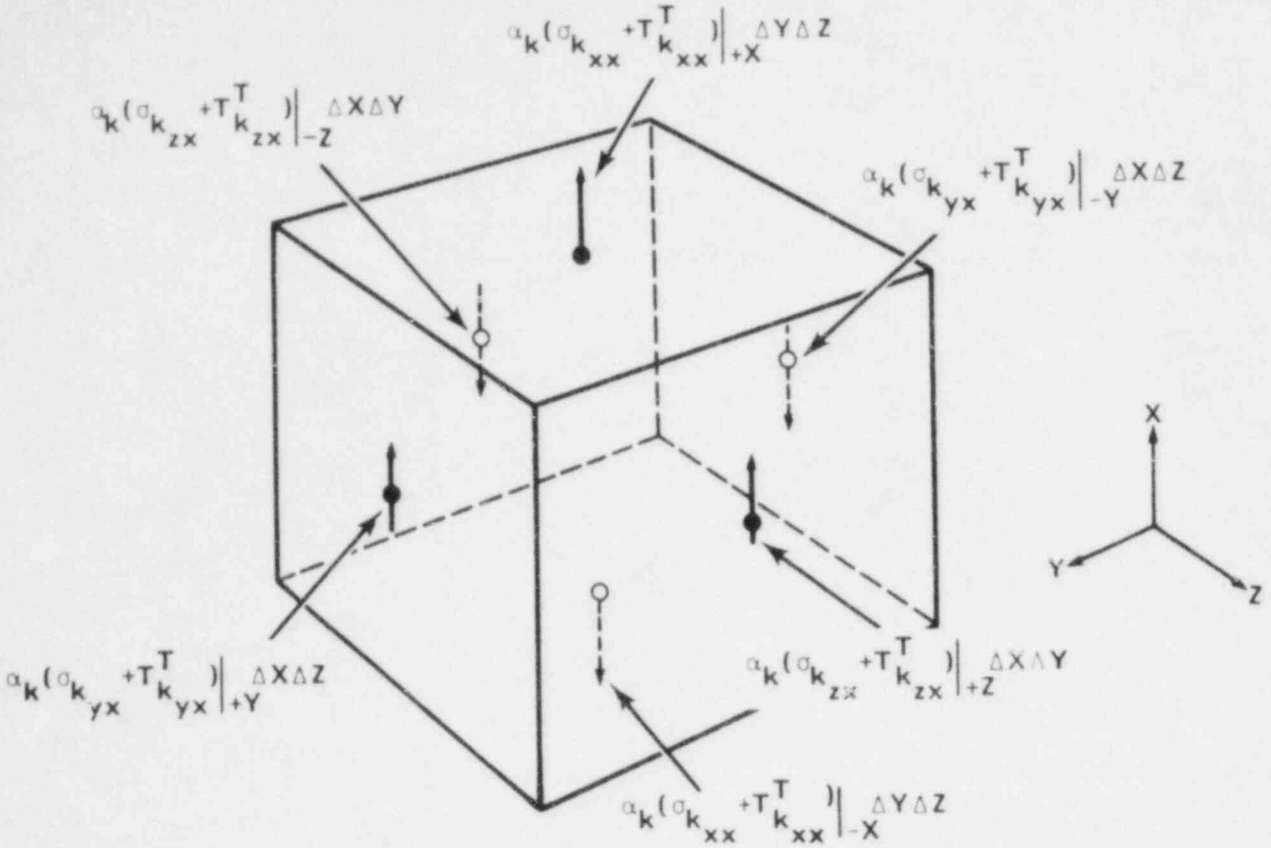

Figure 6 Vertical stresses acting on vertical momentum cell

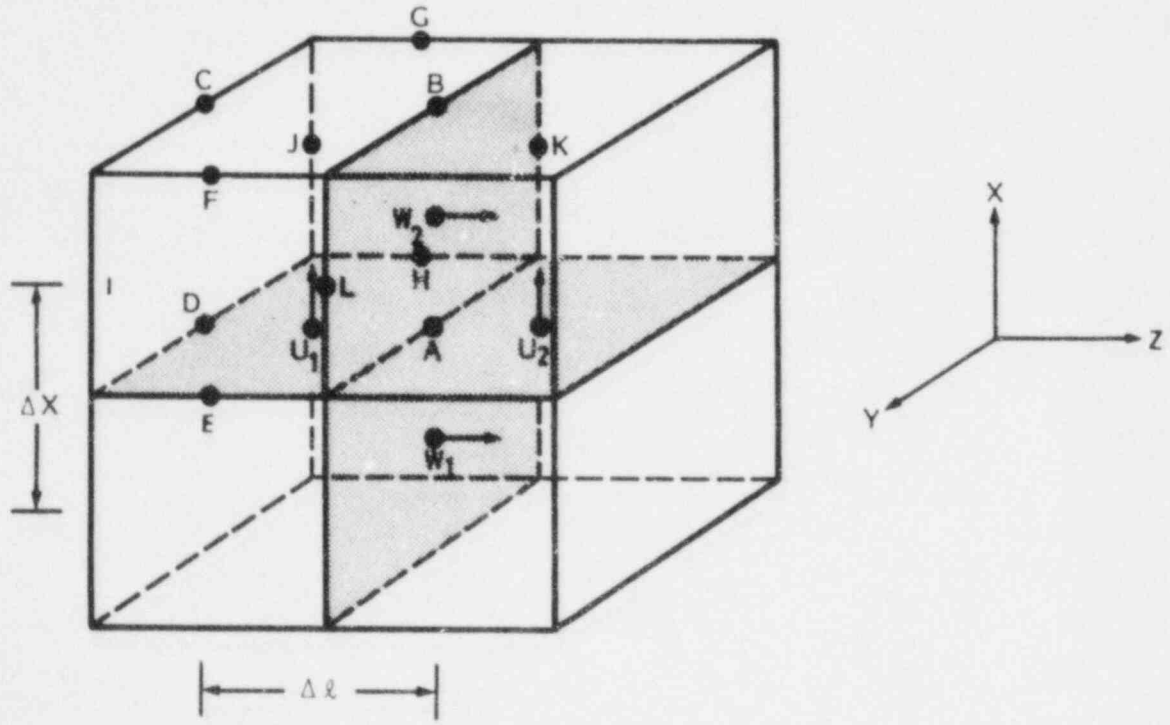

Figure 7 Velocity gradient for point A

The shear stress acting on the sides of the momentum cell is computed from the appropriate velocity gradients calculated on that face. The fluid properties at these locations are computed using a four-point average of the properties in the surrounding four mass cells.

The turbulent mass diffusivity for the mass cell is computed from the double dot product of the deformation tensor and a specified momentum mixing length

$$\epsilon_{D_k} = \ell_m^2 \sqrt{2\underline{\underline{D}}^*_{k_B} : \underline{\underline{D}}^*_{k_B}} \tag{39}$$

Similarly, the turbulent thermal diffusivity for the mass cell center is computed from the double dot product of the deformation tensor

$$\epsilon_k^T = \ell_h \ell_m \sqrt{2\underline{\underline{D}}^*_{k_B} : \underline{\underline{D}}^*_{k_B}} \tag{40}$$

The sum of the conduction and turbulent heat flux between two mass cells is then computed from

$$(q_{k_J} + q^T_{k_J})\big|_{+x} = - \rho_k(\epsilon_k + \epsilon_k^T) \frac{(h_{J+1} - h_{J-1})}{\Delta x_J} \tag{41}$$

The heat fluxes from all surrounding cells are summed to give the net heat flux into cell J.

Because the viscous and turbulent shear stresses are computed explicitly, the time step is limited by the criterion

$$\Delta t \leq \min \left[\frac{1}{\frac{2\ (\mu+\mu^T)}{\rho\ \Delta x^2} + \frac{u}{\Delta x}} \right] \tag{42}$$

4.0 NUMERICAL SOLUTION

The algebraic equations shown in Sections 2.0 and 3.0 form a set that must be solved simultaneously to obtain a solution for the flow fields involved. The numerical scheme chosen to solve these equations must be as efficient as possible to obtain a solution in a reasonable amount of computer time. Although the equations can be solved directly by inversion of the matrix equation, the computer time required for problems with many mesh cells would be prohibitive. By locally reducing the number of equations and unknowns and applying an iterative process to the remaining equations, the sparseness of the global matrix can be utilized and a solution can be obtained in a reasonable amount of computer time. The equations in Sections 2.0 and 3.0 have been greatly simplified over the conservation equations they are intended to represent, because they are written in a semi-implicit form. It is assumed that these semi-implicit equations converge to the correct solution if a time-step size smaller than that required by the Courant criterion is used. The methods used to solve these equations will now be described.

4.1 Solution of the Momentum Equations

The momentum equations are solved first in the solution procedure using currently known values for all of the variables, to obtain an estimate of the new time flow. All explicit terms and variables in the momentum equation are computed in this step and are assumed to remain constant during the remainder of the time step. The semi-implicit momentum equations (Equations 9 through 11 and 16 through 18) have the form:

Liquid

$$F_L = A_1 + B_1 \Delta P + C_1 F_L + D_1 F_V \tag{43}$$

Vapor

$$F_V = A_2 + B_2 \Delta P + C_2 F_L + D_2 F_V + E_2 F_E \tag{44}$$

Entrained Liquid

$$F_E = A_3 + B_3 \Delta P + D_3 F_V + E_3 F_E \tag{45}$$

A_1, A_2, and A_3 are constants that represent the explicit terms in the momentum equations such as the momentum flux terms and the gravitational force. B_1, B_2, and B_3 are the explicit portion of the pressure gradient force term, and C_1^2 and C_2^2 are the explicit factors that multiply the liquid flow rate in the wall and interfacial drag terms. D_1, D_2, D_3, E_2, and E_3 are the corresponding terms that multiply the vapor and entrained liquid flow rates. F_L is the liquid mass flow rate, F_V is the vapor mass flow rate, and F_E is the entrained liquid mass flow rate. These equations may be written in matrix form as

$$\begin{bmatrix} C_1^2 - 1 & D_1 & 0 \\ C_2 & D_2 - 1 & E_2 \\ 0 & D_3 & E_3 - 1 \end{bmatrix} \begin{Bmatrix} F_L \\ F_V \\ F_E \end{Bmatrix} = \begin{Bmatrix} -A_1 - B_1 \Delta P \\ -A_2 - B_2 \Delta P \\ -A_3 - B_3 \Delta P \end{Bmatrix} \tag{46}$$

Equation 46 is solved by Gaussian elimination to obtain a solution for the phasic mass flow rates as a function of the pressure gradient across the momentum cell, ΔP:

$$\begin{aligned} F_L &= G_1 + H_1 \Delta P \\ F_V &= G_2 + H_2 \Delta P \\ F_E &= G_3 + H_3 \Delta P \end{aligned} \tag{47}$$

The mass flow rates given by Equation 47 are computed based on the mass of each phase contained within the momentum control volume. Velocities may be computed from these flow rates using Equation 15. Once the tentative velocities have been obtained from the momentum equations, the continuity and energy equations can be solved.

4.2 Linearization of the Mass and Energy Equations

If the right-hand side of each of the mass and energy equations is moved to the left-hand side, the sum of the terms should be identically equal to zero if the current values of all variables satisfy the equations. The energy and mass equations will not generally be satisfied when the new velocities computed from the momentum equations are used to compute the convective terms in these equations. There will be some residual error in each equation as a result of

the new velocities and changes in the magnitude of some of the explicit terms in the mass and energy equations such as the vapor generation rate. The liquid vapor mass equation, for example, has a residual error given by

$$\frac{[(\alpha_\ell \rho_\ell)_j^n - (\alpha_\ell \rho_\ell)_J]A_{c_J}}{\Delta t} + \sum_{KA=1}^{NA} \frac{[(\alpha_\ell \rho_\ell)^* \tilde{U}_{\ell_j} A_j]_{KA}}{\Delta x_J}$$

$$- \sum_{KB=1}^{NB} \frac{[(\alpha_\ell \rho_\ell)^* \tilde{U}_{\ell_{j-1}} A_{j-1}]_{KB}}{} - \sum_{L=1}^{NKK} S_L \gamma[(\alpha_\ell \rho_\ell)^* \tilde{V}_{\ell_L}]_J$$

$$+ \frac{\Gamma_J}{\Delta x_J} - \frac{S_{C\ell_J}}{\Delta x_J} = E_{CL} \qquad (48)$$

All terms are computed using currently known values for each of the variables. The ~ symbol over the velocities indicates that they are the tentative values computed from the momentum equations (Equation 47). The gas mixture mass equation, the mass equations for the vapor and entrained liquid phases, and the two energy equations also have residual errors: E_{CG}, E_{CV}, E_{CE}, E_{EV}, and E_{EL}. The equations are simultaneously satisfied when E_{CG}, E_{CV}, E_{CL}, E_{CE}, E_{EV}, and E_{EL} for all cells in the mesh simultaneously equal zero. The variation of each of the independent variables required to bring the residual errors to zero can be obtained using the block Newton-Raphson method (Ref. 2). This is done by linearizing the equations with respect to the independent variables αP_g, α_v, $\alpha_v h_v$, $(1-\alpha_v)h_\ell$, α_e, and P to obtain the following equation for each cell of the form

$$[R(X)]\{\delta(X)\} = \{E\} \tag{49}$$

$$[r(X)] = \begin{bmatrix}
\frac{\partial E_{CG}}{\partial \alpha_v P_g} & \frac{\partial E_{CG}}{\partial \alpha_v} & \frac{\partial E_{CG}}{\partial \alpha_v h_v} & \frac{\partial E_{CG}}{\partial (1-\alpha_v)\, h_\ell} & \frac{\partial E_{CG}}{\partial \alpha_e} & \frac{\partial E_{CG}}{\partial P_J} & \frac{\partial E_{CG}}{\partial P_{i=1}} & \cdots & \frac{\partial E_{CG}}{\partial P_{i=NCON}} \\
\frac{\partial E_{CL}}{\partial \alpha_v P_g} & \frac{\partial E_{CL}}{\partial \alpha_v} & \frac{\partial E_{CL}}{\partial \alpha_v h_v} & \frac{\partial E_{CL}}{\partial (1-\alpha_v)\, h_\ell} & \frac{\partial E_{CL}}{\partial \alpha_e} & \frac{\partial E_{CL}}{\partial P_J} & \frac{\partial E_{CL}}{\partial P_{i=1}} & \cdots & \frac{\partial E_{CL}}{\partial P_{i=NCON}} \\
\frac{\partial E_{EV}}{\partial \alpha_v P_g} & \frac{\partial E_{EV}}{\partial \alpha_v} & \frac{\partial E_{EV}}{\partial \alpha_v h_v} & \frac{\partial E_{EV}}{\partial (1-\alpha_v)\, h_\ell} & \frac{\partial E_{EV}}{\partial \alpha_e} & \frac{\partial E_{EV}}{\partial P_J} & \frac{\partial E_{EV}}{\partial P_{i=1}} & \cdots & \frac{\partial E_{EV}}{\partial P_{i=NCON}} \\
\frac{\partial E_{EL}}{\partial \alpha_v P_g} & \frac{\partial E_{EL}}{\partial \alpha_v} & \frac{\partial E_{EL}}{\partial \alpha_v h_v} & \frac{\partial E_{EL}}{\partial (1-\alpha_v)\, h_\ell} & \frac{\partial E_{EL}}{\partial \alpha_e} & \frac{\partial E_{EL}}{\partial P_J} & \frac{\partial E_{EL}}{\partial P_{i=1}} & \cdots & \frac{\partial E_{EL}}{\partial P_{i=NCON}} \\
\frac{\partial E_{CE}}{\partial \alpha_v P_g} & \frac{\partial E_{CE}}{\partial \alpha_v} & \frac{\partial E_{CE}}{\partial \alpha_v h_v} & \frac{\partial E_{CE}}{\partial (1-\alpha_v)\, h_\ell} & \frac{\partial E_{CE}}{\partial \alpha_e} & \frac{\partial E_{CE}}{\partial P_J} & \frac{\partial E_{CE}}{\partial P_{i=1}} & \cdots & \frac{\partial E_{CE}}{\partial P_{i=NCON}} \\
\frac{\partial E_{CV}}{\partial \alpha_v P_g} & \frac{\partial E_{CV}}{\partial \alpha_v} & \frac{\partial E_{CV}}{\partial \alpha_v h_v} & \frac{\partial E_{CV}}{\partial (1-\alpha_v)\, h_\ell} & \frac{\partial E_{CV}}{\partial \alpha_e} & \frac{\partial E_{CV}}{\partial P_J} & \frac{\partial E_{CV}}{\partial P_{i=1}} & \cdots & \frac{\partial E_{CV}}{\partial P_{i=NCON}}
\end{bmatrix}$$

$$\{\delta(x)\} = \begin{Bmatrix} \delta\alpha_v\rho_g \\ \delta\alpha_v \\ \delta\alpha_v h_v \\ \delta)(1-\alpha_v)h_\ell \\ \delta\alpha_e \\ \delta P_J \\ \delta P_{i=1} \\ \vdots \\ \delta P_{i=NCON} \end{Bmatrix} = \{E\} - \begin{Bmatrix} E_{CG} \\ E_{CL} \\ E_{EV} \\ E_{EL} \\ E_{CE} \\ E_{CV} \end{Bmatrix}$$

Det [R(X)] is the Jacobian of the system of equations evaluated for the set of independent variables given by the vector X, δ is the solution vector containing the linear variation of the independent variables, and -E is a vector containing the negative of the residual errors required to bring the error for each equation to zero. The matrix R(X) is composed of analytical derivatives of each of the terms in the equations with respect to the independent variables. The velocities are linearly dependent on the pressures, so derivatives of velocities with respect to pressure may be obtained directly from the momentum equations, Equation 47. The linear variation of velocity with respect to pressure is given by

$$\begin{aligned} \delta V_\ell &= H_1' \ (\delta P_J - \delta P_{J+1}) \\ \delta V_{vg} &= H_2' \ (\delta P_J - \delta P_{J+1}) \\ \delta V_e &= H_3' \ (\delta P_J - \delta P_{J+1}) \end{aligned} \tag{50}$$

The derivatives of the other dependent variables such as ρ_ℓ, ρ_g, ρ_v, h_ℓ, h_f, h_g, and h_v are obtained from the thermal equations of state

$$\rho_\ell = \rho_\ell (P, h_\ell)$$

$$\rho_v = \rho_v (P_v, h_v) \tag{51}$$

$$\rho_g = \rho_g (P_g, h_{mg})$$

and from fundamental identities involving partial derivatives. For example, the derivative of ρ_v with respect to the independent variable $\alpha_v h_v$ is given by

$$\frac{\partial \rho_v}{\partial \alpha_v h_v} = \frac{\partial \rho_v}{\partial h_v} \frac{\partial h_v}{\partial \alpha_v h_v} \tag{52}$$

The derivative $\partial \rho_v / \partial h_v$ is obtained directly from the thermal equation of state, while the derivative $\partial h_v / \partial \alpha_v h_v$ is obtained from the identity

$$h_v = \frac{\alpha_v h_v}{\alpha_v} \tag{53}$$

The term in the numerator is the independent variable with respect to which derivative is being taken, and the denominator is the independent variable α_v which is assumed to be held constant while taking the derivative. From Equation 53 we obtain

$$\frac{\partial h_v}{\partial \alpha_v h_v} = \frac{1}{\alpha_v} \tag{54}$$

Derivatives of the independent variables are obtained directly from Equation 48 and the comparable equations for the other four residual errors. For example, the derivative of the temporal term of Equation 48 with respect to α_v is given by

$$\frac{\partial(\alpha_v \rho_v)}{\partial \alpha_v} = \left(\rho_v \frac{\partial \alpha_v}{\partial \alpha_v} + \alpha_v \frac{\partial \rho_v}{\partial \alpha_v}\right) = \rho_v + \alpha_v \frac{\partial \rho_v}{\partial h_v} \frac{dh_v}{d\alpha_v} = \rho_v - h_v \frac{\partial \rho_v}{\partial h_v} \tag{55}$$

Once all of the derivatives for the five equations have been calculated, Equation 49 is reduced using Gaussian elimination to obtain solutions for the independent variables of the form

$$\delta P_J = a_6 + \sum_{i=1}^{NCON} h_{6_i} \delta P_i \tag{56}$$

$$\delta \alpha_e = a_5 + f_5 \delta \alpha_e + g_5 \delta P_j + \sum_{i=1}^{NCON} h_{5_i} \delta P_i \tag{57}$$

$$\delta[(1-\alpha_v)h_\ell] = a_4 + e_4\, \delta[(1-\alpha_v)h_\ell] + f_4 \delta \alpha_e + g_4 \delta P_J + \sum_{i=1}^{NCON} h_{4_i} \delta P_i \tag{58}$$

$$\delta \alpha_v h_v = a_3 + d_3\, \delta \alpha_v h_v + e_3\, \delta[(1=\alpha_v)h_\ell] + f_3 \delta \alpha_e + g_3 \delta P_J + \sum_{i=1}^{NCON} h_{3_i} \delta P_i \tag{59}$$

$$\delta \alpha_v = a_2 + c_2 \delta \alpha_v + d_2 \delta \alpha_v h_v + e_2 \delta[(1-\alpha_v)h_\ell] + f_2 \delta \alpha_e + g_2 \delta P_J + \sum_{i=1}^{NCON} h_{2_i} \delta P_i \tag{60}$$

$$\delta \alpha_v P_g = a_1 + b_1\, \delta \alpha_v P_g + C_1\, \delta \alpha_v + d_1\, \delta \alpha_v h_v + e_1\, \delta[(1-\alpha_v)h_e]$$

$$+ f_1\, \delta \alpha_e + g_1\, \delta P_J + \sum_{i=1}^{NCON} h_{1_i}\, \delta P_i \tag{61}$$

The computer time required to solve Equation 49 is greatly reduced if the nonlinear coefficients a_k through h_k are assumed to remain constant during a time step and a solution is obtained only for the linearized system of equations (Equations 56 through 61). A substantial savings in computer time is realized when this is done because the matrix equation (Equation 49) is reduced only

once per time step. Time step controls are then imposed to ensure that the variation of the nonlinear terms between time steps remains within acceptable limits so that a stable solution is obtained.

4.3 Solution of the System Pressure Matrix

The linear variation of the pressure in cell J as a function of surrounding cell pressures is given by Equation 56. A similar equation may be derived for each cell in the mesh. This set of equations for the pressure variation in each mesh cell must be simultaneously satisfied. The solution to this equation set may be obtained by direct inversion for problems containing only a few mesh cells or by using a Gauss-Siedel iterative technique for problems containing a large number of mesh cells.

The efficiency of the Gauss-Siedel iteration is increased in two ways. First, direct inversion is carried out over groups of contiguous mesh cells specified by the user. The pressure variations for cells within the group are solved simultaneously while the pressure variations in surrounding mesh cells are assumed to have their last iterate value. A Gauss-Siedel iteration is then carried out over the groups of cells where the pressure variations of bounding cells for each group are updated with their last iterate value. As far as the iterative solution is concerned, solving groups of cells by direct inversion has the effect of reducing a large multidimensional problem to a simpler problem that has the same number of cells as the large problem has groups of cells. Convergence difficulties that are typical of problems with large aspect ratios (long, narrow cells) are also eliminated by placing cells with large aspect ratios between them within the same solution group. The iteration is assumed to have converged when the change in linear pressure variation between time steps is below a specified limit.

The second method for increasing the efficiency of the iteration involves the calculation of an initial estimate for the pressure variation in each cell. This is done through a process called rebalancing. Rebalancing is simply the process of reducing the multidimensional mesh to a one-dimensional mesh for the vessel and then obtaining a solution for the pressure variation at each level of the one-dimensional problem by direct inversion using the methods described above. The one-dimensional solution for the linear pressure variation at each level is then used as an initial guess for the linear pressure variation in each mesh cell on that level in the multidimensional problem. This process greatly enhances the rate of convergence in many problems because the one-dimensional solution generally gives a good estimate for the magnitude of the linear pressure variation in the multidimensional problem. Rebalancing is optional and must be specified by the user. If this option is not used, then the initial guess for the linear pressure variation in each cell is zero.

4.4 Unfolding of Independent and Dependent Variables

Once a solution for the linear pressure variation in each cell has been obtained, the linear variation in the other independent variables is unfolded

using Equations 57 through 60. The new value for each of the independent variables is then updated as follows:

$$
\begin{aligned}
P^n &= P + \delta P \\
\alpha_v^n &= \alpha_v + \delta\alpha_v \\
\alpha_e^n &= \alpha_e + \delta\alpha_e \\
(\alpha_v h_v)^n &= \alpha_v h_v + \delta\alpha_v h_v \\
[(1-\alpha_v)h_\ell]^n &= (1 - \alpha_v)h_\ell + \delta(1 - \alpha_v)h_\ell \\
(\alpha_v P_g)^n &= \alpha_v P_g + \delta\alpha_v P_g
\end{aligned}
\tag{62}
$$

The new time liquid volume fraction is simply $\alpha_\ell^n = 1.0 - \alpha_v^n - \alpha_e^e$.

The dependent variables P_g, h_v, and h_ℓ are calculated as follows:

$$
\begin{aligned}
P_g^n &= \frac{(\alpha_v P_g)^n}{\alpha_v^n} \\
h_v^n &= \frac{(\alpha_v h_v)^n}{\alpha_v^n} \\
h_\ell^n &= \frac{[(1 - \alpha_v)h_\ell]^n}{(1 - \alpha_v^n)} \\
h_{mg}^n &= h_{mg} + \frac{C_{P_g}^n}{C_{P_v}^n}(h_v^n - h_v)
\end{aligned}
\tag{63}
$$

The new time steam pressure is obtained as follows:

$$p_s^n = p^n - p_g^n \tag{64}$$

The new time densities are then obtained from the equations of state

$$\rho_v^n = \rho_v(p_s^n, h_v^n)$$

$$\rho_\ell^n = \rho_\ell(p^n, h_\ell^n)$$

$$\rho_g^n = \rho_g\ (p_g^n, h_g^n)$$

The velocities are then updated by

$$V_k^n = V_k + \delta V_k \tag{65}$$

where δV_k is given by Equation 50.

4.5 Time Step Control

Checks are made on the value of each of the new time variables to ensure that the variation of the new time variables from the old falls within reasonable limits. If the new time variables have nonphysical values (e.g., void fractions less than zero or greater than 1.0) or if the variation of the new time variable from the old is unreasonably large, then the solution is backed up to the beginning of the time step, the variables are set to their old time value, the time step is halved, and the time step is repeated. This is done so that the linearized equations will be sufficiently representative of the nonlinear equations to provide an acceptable level of accuracy in the calculation. The time step size is also controlled by the rate of change of the independent variables for the same reason. The stability of the solution is further enhanced by using logarithmic damping between the old and new time values of some of the explicit terms. In particular, the interfacial drag and heat transfer coefficients are damped according to

$$\chi^n = \tilde{\chi}^{(1,ex)} \cdot \chi^{ex} \tag{66}$$

where ex is a user-specified damping exponent usually set to $0.7 \leq ex \leq 0.9$.

RELATED DOCUMENTS

COBRA/TRAC - A Thermal Hydraulics Code for Transient Analysis of Nuclear Reactor Vessels and Primary Coolant Systems, NUREG/CR-3046, March 1983

Volume 1: Equations and Constitutive Models

Volume 2: Numerical Solution Methods

Volume 3: Users' Manual

Volume 4: Developmental Assessment and Data Comparison

Volume 5: Programmers' Manual

COBRA-NC: A Thermal-Hydraulic Code for Transient Analysis of Nuclear Reactor Components

Volume 1: Equations and Constitutive Models NUREG/CR-3262

Volume 2: Numerical Solution Methods NUREG/CR-3262

Volume 3: Users' Manual for General Two-Phase Thermal Hydraulics (to be published)

Volume 4: Users' Manual for Containment Analysis (COBRA-NC), NUREG/CR-3262

Volume 5: Users' Manual for Flow Blockage and Hot Bundle Analysis (to be published)

Volume 6: Assessment Manual for General Two-Phase Thermal-Hydraulic Applications (to be published)

Volume 7: Assessment Manual for Containment Applications, NUREG/CR-3262

Volume 8: Assessment Manual for Flow Blockage and Hot Bundle Applications (to be published)

Volume 9: Programmers' Manual (to be published)

5.0 REFERENCES

1. D. R. Liles et al. IRAC-PD2 An Advanced Best-Estimate Computer Program for Pressurized Water Reactor Loss-of-Coolant Accident Analysis, NUREG/CR-2054, U.S. Nuclear Regulatory Commission, Washington, D.C., April 1981.

2. D. R. Liles and W. H. Reed, 1978. "A Semi-Implicit Method for Two-Phase Fluid Dynamics." J. of Comp. Physics 26 (3), 390-407.

NUREG/CR-3262
PNL-5515
Vol. 2
R4

DISTRIBUTION

No. of Copies

OFFSITE

U. S. Nuclear Regulatory Commission
Division of Technical Information and Document Control
7920 Norfolk Avenue
Bethesda, MD 20014

20 Tim Lee
Analytical Model Branch
Office of Nuclear Regulatory Research
U. S. Nuclear Regulatory Commission
7915 Eastern Avenue
MS-1130-SS
Washington, DC 20555

No. of Copies

ONSITE

50 Pacific Northwest Laboratory

CL Wheeler (43)
Publishing Coordination (2)
Technical Information (5)

NRC FORM 335 (2-84) NRCM 1102, 3201, 3202

U.S. NUCLEAR REGULATORY COMMISSION

BIBLIOGRAPHIC DATA SHEET

SEE INSTRUCTIONS ON THE REVERSE

1. REPORT NUMBER (Assigned by TIDC, add Vol. No., if any)
NUREG/CR-3262
PNL-5515
Vol. 2

2. TITLE AND SUBTITLE
COBRA-NC: A Thermal-Hydraulic Code for Transient Analysis of Nuclear Reactor Components, Volume 2: COBRA-NC Numerical Solution Methods

3. LEAVE BLANK

4. DATE REPORT COMPLETED
MONTH: March YEAR: 1986

5. AUTHOR(S)
M. J. Thurgood, T. L. George, C. L. Wheeler

6. DATE REPORT ISSUED
MONTH: April YEAR: 1986

7. PERFORMING ORGANIZATION NAME AND MAILING ADDRESS (Include Zip Code)
Pacific Northwest Laboratory
PO Box 999
Richland, WA 99352

8. PROJECT/TASK/WORK UNIT NUMBER

9. FIN OR GRANT NUMBER
B2466

10. SPONSORING ORGANIZATION NAME AND MAILING ADDRESS (Include Zip Code)
Division of Accident Evaluation
Office of Nuclear Regulatory Research
U. S. Nuclear Regulatory Commission
Washington, D. C. 20555

11a. TYPE OF REPORT
Technical Report

b. PERIOD COVERED (Inclusive dates)

12. SUPPLEMENTARY NOTES

13. ABSTRACT (200 words or less)

The COBRA-NC computer program has been developed to predict the thermal-hydraulic response of nuclear reactor components to thermal-hydraulic transients. The code solves the multicomponent, compressible three-dimensional, two-fluid, three-field equations for two-phase flow. The three fields are the vapor field, the continuous liquid field, and the liquid drop field. The code has been used to model flow and heat transfer within the reactor core, the reactor vessel, the steam generators, and in the nuclear containment. This volume describes the finite-volume equations and the numerical solution methods used to solve these equations. It is directed toward the user who is interested in gaining a more complete understanding of the numerical methods used to obtain a solution to the hydrodynamic equations.

14. DOCUMENT ANALYSIS - a. KEYWORDS/DESCRIPTORS
a. Keywords/Description
COBRA-NC, Containment analysis
3-D Finite Difference Code
2-Ø, 3-Fields, Compressible Flow
Numerical Solution Methods

b. IDENTIFIERS/OPEN-ENDED TERMS

15. AVAILABILITY STATEMENT
Unlimited

16. SECURITY CLASSIFICATION
(This page) Unclassified
(This report)

17. NUMBER OF PAGES

18. PRICE